2023 IEEE/ASME International Conference on Advanced Intelligent Mechatronics (AIM)
June 28-30, 2023. Seattle, Washington, USA

ARMoR: Amphibious Robot for Mobility in Real-World Applications

Matthew G. Hammond
Process Automation & Controls Group
Los Alamos National Laboratory
Los Alamos, New Mexico, USA
matthammond@lanl.gov

Kiju Lee
Engineering Technology & Industrial Distribution
Mechanical Engineering, Texas A&M University
College Station, Texas, USA
kiju.lee@tamu.edu

***Abstract*—This paper presents a mobile robot for amphibious surface locomotion called ARMoR. The locomotion system of ARMoR consists of two wheel-and-leg transformable mechanisms and a customizable balancing tail. A sphere body chassis containing electronic components assembles the wheels and the tail. A combination of chassis design and transformable wheels allows ARMoR to safely navigate various environments, including diverse terrains and water surfaces. The robot is controlled and operated using an embedded microprocessor interfacing with sensing, communicating, and powering modules, including the Global Positioning System (GPS), camera, Inertial Measurement Unit (IMU), wireless communication module, and batteries. ARMoR was tested for its locomotion capabilities on concrete, dirt, grass, rocky surface, low brush, stairs, and water. On concrete, dirt, and grass, ARMoR operated in the wheeled mode; on other surfaces, the wheels transformed into the legged configuration enabling the robot to traverse challenging surface conditions effectively. ARMoR successfully traversed all terrains, and the traversal speeds were measured.**

***Index Terms*—Mobile robots, amphibious locomotion, ground robots, wheeled robot locomotion**

I. Introduction

ARMOR, the Amphibious Robot for Mobility in Real-world applications, is developed as a simple, cost-effective solution for autonomous navigation on diverse terrains. The robot is designed to be modular, consisting of a sphere body chassis, two wheels, and a tail, allowing customization of each module depending on required mobility and embedded payloads. As shown in Fig. 1, the robot has two transformable wheels based on the WheeLeR mechanism's design [1]. This mechanism consists of a central gear connected to the driving motor and a set of leg segments, which can open under high friction or when encountered by an obstacle. It is a passive mechanism without any additional actuator for opening and closing the legs; instead, the mechanism dynamically changes its configuration, adapting to the surface conditions. While the number of leg segments is customizable, we selected the 4-leg design for ARMoR, which showed high climbability and reliable performance on other surfaces [2].

While our previous works [1], [2] focused on achieving multi-terrain locomotion, this paper extends the robot's operation space to terrain and water surfaces without increasing the structural or control complexity involved with the robot's operation. This requires the robot to maintain the passive

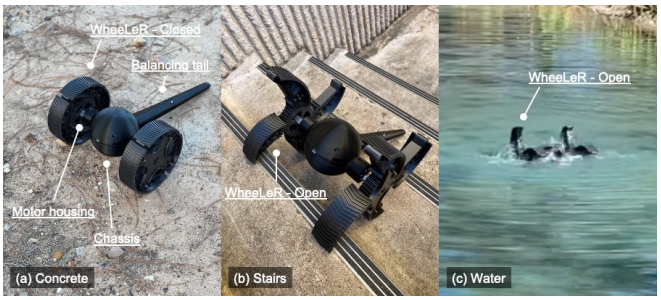

Fig. 1. ARMoR with passively transforming wheels on (a) concrete, (b) stairs, and (c) water surface.

nature of the transformable wheels, enabling these wheels to effectively propel the robot on a water surface, sealing the robot to be water resistant, and keeping the overall structural complexities as simple as possible. While the overall mechanical structure benchmarks the previous proof-of-concept prototype [1], ARMoR is a fully functional robot with the necessary sensing, computing, communication, and powering components.

We also note that ARMoR is developed as part of the project establishing a scalable and configurable robotic swarm system for agriculture funded by the National Institute of Food and Agriculture (NIFA) in the United States Department of Agriculture (USDA). This project aims to develop a swarm of low-cost robotic agents to perform diverse agricultural tasks collaboratively. Therefore, low cost and simplicity in software and hardware were important criteria for developing ARMoR. In addition, the embedded computing and communication devices were selected to interface with other robots in the swarm easily.

Related Works

Achieving real-world mobility is difficult for small-size mobile robots [3]. Many robots, therefore, target a specific environment or a subset of terrains for particular applications [4], [5]. Versatile mobility to navigate different environments can greatly expand the utility of mobile ground robots, particularly for applications in hazardous environments [6]–[8]. To advance mobility beyond wheels–most commonly adopted for ground locomotion, some robots use mechanisms that

can transform into different configurations. The transformation may be active, using additional motors or actuators, or passive, taking advantage of geometry and mechanical properties to transform the shape of the robot's wheels. Various active and passive mechanisms have been introduced, including actuator-driven transformations and origami-inspired designs [1], [10]–[13]. The changes in shapes and dimensions allowed these robots to overcome large obstacles or traverse rough terrains [1], [14]. Improved mobility often requires high-torque motors capable of lifting the robot's weight over obstacles. These motors must balance speed with motor torque so that the robot can move as quickly as possible while still being able to traverse obstacles [15]. Such operation is often implemented using closed-loop systems, such as PID control, whose feedback allows the robot to actively monitor its output and compensate for any difference between that and the input signal [16]–[19].

Sensory capabilities are also integral to a robot's ability to navigate real-world environments to avoid hazards and collect environmental data for study or decision-making [7], [8], [20]. The ability to monitor battery metrics also allows mobile robots to be more practical in the real-world [13], [21]. The battery life and health status can be used to determine its likelihood of success at a given task and when it should return to a charging station autonomously [13]. This makes the robots much more reliable in unpredictable environments and reduces the chance of power loss during operation [22].

The rest of the paper is organized as follows. Section II details the mechanical design, and Section III describes the electrical design of ARMoR. Locomotion experiments and results are presented in Section IV.

II. Mechanical Design

ARMoR's mechanical design focuses on the cost, scalability, and modularity necessary for future swarm implementation and the resiliency and versatility required for real-world operation.

A. Chassis Design

The robot's chassis, an exploded view shown in Fig. 2, consists of eight major components. Each of these components is fabricated using 3D printing, aiming to facilitate design iteration, customization, and convenience of additive manufacturing. Excluding the tip of the tail, all pieces are 3D-printed using Polylactic Acid (PLA) filament. PLA has a high strength-to-weight ratio and is inherently resistant to both water and earthly temperature extremes, making it an effective choice for the robot operating in outdoor environments. Furthermore, PLA is relatively inexpensive and easy to acquire worldwide, making it an effective choice for scalable robotic swarms. The tip of the tail is manufactured using Thermoplastic Polyurethane (TPU) filament for flexibility and high friction to support the robot when attempting to climb obstacles properly.

The main housing contains all of the robot's electrical components and has a spherical profile. The sphere shape of the main body reduces the impact force experienced by the robot's internal parts because it tends to allow other objects to glance or slide off of its surface instead of directly delivering the impact force. The main sphere body consists of three parts, an upper casing, a lower casing, and a central platform where most electrical components are mounted. The central platform is also designed with two cylindrical motor housings that secure and protect the robot's high-torque motors during operation. Each motor is also covered with a motor cap to protect it from environmental hazards. These caps have six mounting holes for the motor's mounting screws and a larger seventh hole from which the motor's axle extrudes. These caps are rotationally locked using a slot element that fits around a rectangular protrusion located on the cylindrical portions of the central platform.

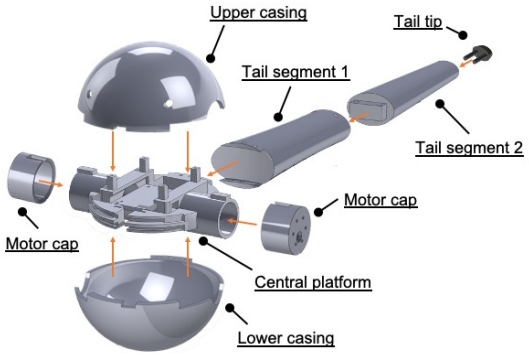

Fig. 2. Exploded view of the ARMoR chassis consisting of the central platform top and bottom sphere cases, two motor housing parts, two tail segments, and a tail tip.

The final three components make up the tail portion. The base of the tail encompasses protruding elements from the upper casing, central platform, and lower casing, as well as the three central screws used to secure each of these components. This joint allows for easy disassembly of the robot during maintenance or recharging. The secondary tailpiece allows the tail as a whole to be modular so that its length or shape can be modified more quickly using less material. The tail tip serves as the robot's third point of contact with the ground and provides it with balance during locomotion on flat ground or while scaling obstacles. The length of each tail segment can be customized depending on the mobility requirements, particularly for projected obstacle heights. This modular tail design may be replaced with a linear linkage where the length can be manually set or autonomously adjusted with an embedded actuator.

B. Transformable Wheel Design Modification

As stated earlier, ARMoR's wheels are based on the transformable wheel design, WheeLeR [1]. These wheels can change their configurations between wheels and legs, facilitating flexible mobility and climbing. The main mechanism of these wheels consists of a central driving gear and several toothed leg components that serve as the driven gears in the system. These components and the spoked frames holding all

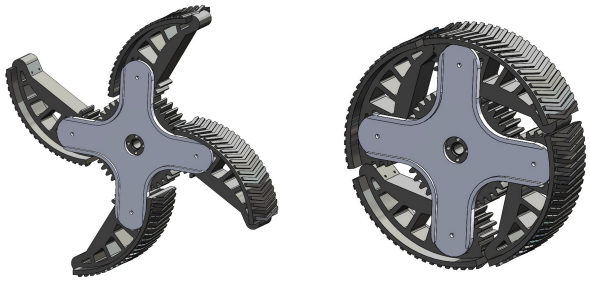

Fig. 3. CAD models of the passively transformable wheels used in ARMoR: closed wheel configuration (left) and open leg configuration (right).

parts together are secured to the motor shaft by a mechanical wheel hub. Fig. 3 shows the CAD models of the wheel in two different configurations. The gear ratio used for these wheels is empirically optimized such that the friction of the wheel's contact with flat surfaces (e.g., concrete, asphalt, and low grass) does not cause them to transform into the open leg configuration. This feature allows ARMoR to capitalize on the advantages of wheels – the most smooth, energy-efficient method of locomotion on relatively flat and smooth surfaces. When ARMoR encounters rough terrains or obstacles, the increased frictional force overcomes the torque limit of the wheel's gear ratio, causing them to transform into the open-legged configuration. This allows ARMoR to use the geometric advantages of legs for scaling obstacles that it would otherwise be unable to surmount.

The final wheel design selected for ARMoR consists of six major components fabricated using the same 3D-printing method and material (i.e., PLA) as the chassis. The robot's driving motor shaft is connected to the central gear through a mechanical wheel hub. The four toothed leg components assembled around the central gear serve as both the acting surface of the wheel configuration and the legs of the open configuration. The rolling surface of each toothed leg has treads to increase traction and overhangs to improve their ability to provide locomotion in the water. The final piece of the wheels is the support bracket, which maintains ideal interaction between the gear pieces. This ensures that they operate effectively and stay engaged in the field.

C. Waterproofing Methods and Aquatic Considerations

The primary functional improvement in ARMoR over our previous works is its capability of water surface locomotion. The hydrodynamic profile and the transformable wheels make ARMoR well-suitable for amphibious locomotion. ARMoR is designed to operate on the surface of the water. This allows the platform's design to maintain simplicity and introduces a minimum buoyancy threshold for ARMoR to float in water. Subsurface operation requires controlling the robot's buoyancy in addition to associated sensors and other components that significantly increase the mechanical, electrical, and control complexities.

ARMoR is insulated in such a way so that there is only negligible water infiltration within the main housing, ensuring that the internal components remain intact. Insulation is accomplished through a combination of design choices and additional measures that work together. The spherical profile of ARMoR's main housing has relatively few seams, minimizing the infiltration points for water during aquatic operation. Each seam is also designed to be a complex connection, reducing the chance of seepage from the outside. These seams are then reinforced using a number of traditional waterproofing methods, including foam weatherstrip, waterproof epoxy, and waterproof tape. Additional layers of waterproof tape can also be added to the exterior of the main housing to reinforce the barrier to external water further.

For ARMoR to remain on the water surface and avoid the higher levels of pressure and uncertainty associated with the subsurface operation, it must be buoyant enough to float freely. This buoyancy results from three distinct design choices introducing air pockets into the structural design. This excessive air reduces the robot's overall density and decreases the buoyant force necessary for proper flotation. The first air pocket introduced into the design is that encompassed by the main housing. This housing is designed to resist water infiltration, meaning all empty space within the cavity is filled with buoyant air. The air pocket exists within the solid components of the wheels and tail. These empty spaces increase flotation without compromising the structural integrity of the part. The third air pocket in the design results from the 3D-printing method. The infill rate used for printing was calibrated to 20%. This reduces the overall weight and density of the parts while maintaining their strength and rigidity. An optional life jacket was also designed to allow ARMoR to sit higher in the water for improved efficiency during aquatic locomotion when needed. The jacket uses polyethylene foam and is highly buoyant, decreasing ARMoR's subsurface interactions.

III. Electrical Design

This section describes the robot's electrical design with a power/battery management system and embedded sensors for navigation and communication.

A. Power Flow and Battery Management

Battery life is an important consideration for any mobile robot as it is a major limitation on their ability to operate effectively. To allow ARMoR to monitor the battery level and thus properly plan its operation, we equipped ARMoR with an onboard Battery Management System (BMS). BMS tracks a battery's charge level, discharge rate, and overall health. BMS is connected directly to the robot's main 12V battery and is capable of monitoring Lithium Ion (LiIon), Nickel Cadmium (NiCd), Lead Acid (PbA), and Nickel Metal Hydride (NiMH) battery chemistries. ARMoR uses a 2200 mAh NiMH battery due to its steady discharge rate and voltage.

ARMoR's internal power circuit is shown in Fig. 4. The main 12 V battery supplies power to the platform's high-torque motors, and a supplemental battery powers the 5V components. In the event of a malfunction in the supplemental battery circuit, ARMoR can also supply 5V using a power

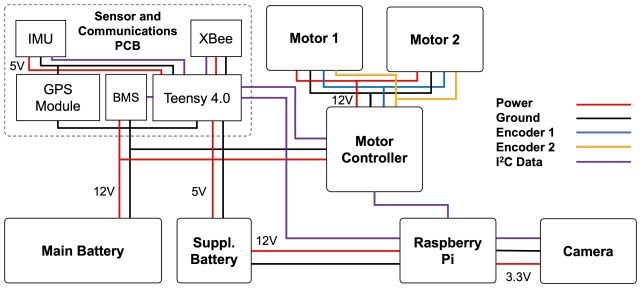

Fig. 4. Electronic components with double battery design.

regulation circuit built into the motor controller. This circuit uses the 12V input from the main battery and steps it down to the 5V required by the robot's sensors and computing and communication devices. The main battery can power up to 150 minutes of maximum-speed operation and 240 minutes when operated at about 50% of the maximum speed. The supplemental battery gives the motors and motor controller – capable of drawing upwards of 300 mA of current under high torque conditions – approximately 45 additional minutes of operating time. The maximum current draw of each component has been checked against the amperage ratings of the main battery, supplemental battery, and the voltage regulators on the motor controller to ensure that each component can meet the demands of the components that it is powering.

B. Sensor Integration and Communication

Sensors provide robots with the ability to perceive their environment and are integral to performing diverse tasks. ARMoR is equipped with four primary sensors for effectively navigating in various environments. The Internal Measurement Unit (IMU) and the Global Positioning System (GPS) module provide ARMoR with location and orientation data. The IMU can determine the linear velocity, acceleration, and relative robot orientation. The symmetrical design of the robot's chassis allows the robot to operate upside down, and the IMU can determine the robot's physical status for applying a suitable control scheme. This feature can be particularly useful for space-constrained environments. The other two sensors integrated into ARMoR's design are the BMS described above, which monitors battery metrics, and a camera module located on the front of the robot. The camera with implemented computer vision algorithms allows ARMoR to perceive its operating environment and make autonomous decisions. Operators can teleoperate or actively monitor a robot's process using a video feed or look back after the robot completes the operation.

The IMU, GPS, and BMS are integrated into the ARMoR platform using a Printed Circuit Board (PCB). This PCB also houses the XBee module, which uses the ZigBee-based protocol to communicate with other nodes or a host device through radio wirelessly. Zigbee communication is low-cost and effective for robot-to-robot communication, especially when many robots are expected to communicate and collaborate with each other. This allows ARMoR to support a scalable mesh network, allowing robots to relay communications far beyond their individual signal ranges. ARMoR's camera module is connected using external serial connections to promote modularity within the design. Therefore, the camera module is interchangeable and can be replaced with minimal rewiring. A multitude of additional ports on the main processing board (i.e., Raspberry Pi) allows users to further customize ARMoR's sensory and functional capabilities.

C. Motor Performance Analysis

ARMoR's amphibious locomotion capabilities are supported by the combination of transformable wheels and high-torque motors. While a conventional hardware development process would start with a motor selection based on the weight and payload estimation and required functional criteria, we started with a specific type of motor serving as the hardware constraint and designed the rest to meet the locomotion requirements. This motor has a gear ratio of $131.25:1$ and a maximum torque rating of $45kg\text{-}cm$. For the robot to traverse diverse terrains and overcome obstacles (including stairs), two of these motors must provide sufficient torques for lifting the entire body with the support of the tail, resulting in a moment arm length of $108mm$ when ARMoR's wheels are closed and $170mm$ when they are open. These values can be used in the relationship

$$\tau = rF\sin\theta$$

to determine the maximum allowable weight of the ARMoR platform.

While the wheel's angle of contact with the ground is approximately 90°, we cannot always guarantee this considering the transformable nature of the wheels. We used 80°, considering a tolerance of $\pm 10°$. This value exceeds the predicted average of the wheel's contact angle variations, introducing a factor of safety into the calculations. A conversion factor of 0.098 is also included to facilitate the conversion from $kg\text{-}cm$ to Nm; the $170mm$ moment arm is chosen to represent the maximum load on the motor. Then, the weight limit of ARMoR based on the two-motor design is calculated as $2 \cdot 45 \cdot 0.098 = 170 \cdot F \cdot \sin 80°$, resulting in $F = 52.683N$.

The mass of the constructed robot was $2.703kg$. Based on the equation $F_G = mg$ where m is the mass and g is the gravitational acceleration, the gravitational force experienced by ARMoR is estimated as $F_G = 26.516N$. A factor of safety can then be calculated using the ratio of the motor's maximum torque rating to the weight of the robot, such that $F/F_G = 1.987$. The motors have a factor of safety of two, relative to the robot's weight. This means that the motors will provide sufficient torques to lift the robot, allowing it to scale large obstacles and stairs.

IV. Locomotion Experiments

Testing ARMoR's mobility involved various terrains and a water surface shown in Fig. 5. Locomotion performance on each surface was measured by run time, success rate, and average speed.

Fig. 5. Locomotion testing environments including concrete, dirt, grass, rocks, low brush, stairs, and water.

A. Experimental Settings and Measures

The primary mode of testing involved repeated ten-meter trials across seven different terrain types: concrete, dirt, grass, rocks, low brush, stairs, and water. During each of these trials, the time taken for ARMoR to reach the ten-meter mark was recorded and later used to calculate the average rotational velocity of the motors for each terrain type. On each surface, ARMoR was remotely controlled to move $10m$ forward three times at two different speed settings: 65 rpm and 80 rpm. These two rotational speeds refer to the target speed sent as an input signal to the motors, not the actual rotational velocities, and they represent 80% and 100% of the motor's maximum rotational velocities, respectively. The time for traversing a $10m$ distance was measured from each trial. The times from the three for each input and terrain combination were first averaged and then used to determine the average linear velocity (v) for that terrain and input using $v = t_{ave}/d$, where t_{avg} is the average time, and d is the $10m$ distance. Then, the linear velocity is converted to the actual rotational velocity of the motor, such that

$$\omega = 60v/C,$$

where C is the wheel's circumference, ω is the actual rotational velocity of the motor, and 60 is multiplied by v for per-minute speed. The wheel circumference is obtained using either the closed-wheel configuration radius or the open-legged configuration radius, depending on the configuration utilized on each terrain.

B. Results

ARMoR successfully traversed all environments considered for locomotion testing in all trails. Table I shows the average time for $10m$ terrain testing obtained from three 65 rpm trails and three 80 rpm trials on each terrain. The resulting terrain-specific rotational velocities are also summarized in Table II with the same terrain and input velocity labels. On relatively flat and smooth surfaces, including concrete, dirt, and grass, the $10m$ traversal time was short, and the motor input speed closely matched the actual output rotational speed. ARMoR took longer to traverse the same distance on rocks and low brush. The actual output speed was about 75% (65 rpm) and 65% (80 rpm) of the input speeds on rocks and 84% (65 rpm) and 74% (80 rpm) on low brush. On stairs and a water surface, the robot's speed was significantly dropped in both speed settings. However, ARMoR showed reliable locomotion performance in these two challenging conditions. On concrete, dirt, and grass, the wheels remained closed in all trials. On rocks, low brush, stairs, and water surfaces, the wheels transformed into the legged configuration and remained open while traversing those surfaces.

TABLE I
10-METER TERRAIN TESTING TIMES IN SECONDS

Terrain Type	65 rpm trials			80 rpm trials		
	1	*2*	*3*	*1*	*2*	*3*
Concrete	13.7	14.1	13.8	12.2	12.4	12.5
Dirt	14.2	14.2	13.9	13.8	13.9	13.9
Grass	14.5	14.9	14.4	13.9	14.1	13.8
Rocks	18.9	18.4	17.2	16.4	17.9	16.2
Low Brush	15.8	16.7	16.0	15.4	15.0	14.4
Stairs	36.5	43.0	39.5	38.0	37.0	40.5
Water	32.2	37.7	39.8	29.9	39.5	31.4

TABLE II
TERRAIN SPECIFIC ROTATIONAL VELOCITIES IN RPM

Terrain Type	65 rpm input	80 rpm input
Concrete	63.8	71.5
Dirt	62.7	63.8
Grass	60.6	63.5
Rocks	48.7	52.5
Low Brush	54.7	59.2
Stairs	22.3	23.0
Water surface	24.2	26.3

V. CONCLUSION AND DISCUSSION

Many existing mobile robots tend to be either small and fragile with limited real-world practicality or bulky and expensive with little flexibility and scalability. ARMoR is a two-wheeled mobile robot that prioritizes agility, compact design, low weight, robustness, and cost efficiency. ARMoR's robust design and versatile motion lend the robot to real-world applications that would often not be feasible for small robots. The transformable wheels used for ARMoR could shift from a circular wheel shape to a four-legged configuration when sufficient frictional force was experienced. The modified wheel design also allowed it to catch water on a series of exposed flanges providing effective locomotion on water surfaces. ARMoR's amphibious mobility promises a broad range of applications, including agriculture, search-and-rescue, and space exploration.

The ARMoR platform will continue to improve over time as the hardware is fine-tuned and integrated with autonomous control. This, coupled with the implementation of intelligent

control and autonomous navigation algorithms, will result in a functional robotic platform that can operate in the real world. An extended work that would be valuable for future use would be the exploration of other manufacturing methods. 3D printing in PLA was selected due to its balance between material properties and convenience, but that does not mean that it is the best option. The current chassis is acceptable for water surfaces, but the porous nature of the printed structures makes it susceptible to water infiltration when the body is submerged in water or on the water surface for an extended time. Further experiments will be required to better understand the relationships among the material, 3D printing infill rate, and wall thickness. Additional post-processing may also be applied to the printed parts, such as acetone vapor smoothing, which is known to help with waterproofing. Wheel designs with an emphasis on hydrodynamics may also improve ARMoR's aquatic locomotion capabilities, and new tread materials may allow it to better climb stairs or other large obstacles.

ACKNOWLEDGMENT

The hardware development of this project was supported by the National Institute of Food and Agriculture, United States Department of Agriculture (USDA-NIFA), Award No. 2021-67021-35959 (PI: K. Lee). This project was performed while M. Hammond was with the Department of Engineering Technology & Industrial Distribution at Texas A&M University, and he is currently with Los Alamos National Laboratory, which has approved this paper for public release (LA-UR-23-24845).

REFERENCES

[1] Zheng, C., & Lee, K. (2019). "WheeLeR: Wheel-leg reconfigurable mechanism with passive gears for mobile robot applications," In Proceedings of *IEEE International Conference on Robotics and Automation (ICRA)* (pp. 9292-9298). IEEE.

[2] Zheng, C., Sane, S., Lee, K., Kalyanram, V., & Lee, K. (2023). "α-WaLTR: Adaptive Wheel-and-Leg Transformable Robot for Versatile Multiterrain Locomotion," in *IEEE Transactions on Robotics*, vol. 39, no. 2, pp. 941-958.

[3] Yamada, Y., Miyagawa, Y., Yokoto, R., & Endo, G. (2015). "Development of a Blade-Type Crawler Mechanism for a Fast Deployment Task to Observe Eruptions on Mt. Mihara," *Field Robotics*. 33, 371–390.

[4] Farritor, S., Dubowsky, S., Rutman, N., & Cole, J. (1996). "A systems-level modular design approach to field robotics," In Proceedings of *IEEE International Conference on Robotics and Automation* (Vol. 4, pp. 2890-2895). IEEE.

[5] Akers, E. L., Harmon, H. P., Stansbury, R. S., & Agah, A. (2004). "Design, fabrication, and evaluation of a mobile robot for polar environments," In IGARSS 2004. *IEEE International Geoscience and Remote Sensing Symposium* (Vol. 1). IEEE.

[6] Bidaud, P. (2011). Field Robotics: Proceedings of the *14th International Conference on Climbing and Walking Robots and the Support Technologies for Mobile Machines*, University Pierre Et Marie Curie (UPMC), Paris France.

[7] Lynch, K. & Park, F. (2019). Modern Robotics: Mechanics, Planning, and Control. Cambridge University Press.

[8] Craig, J. (2004). Introduction to Robotics: Mechanics and Control. Pearson.

[9] Nagatani, K., Kuze, M., & Yoshida, K. (2007). "Development of transformable mobile robot with mechanism of variable wheel diameter," *J. Robot. Mechatron,* 19(3), 252-257.

[10] She, Y. Hurd, C. & Su, H. (2015). "A transformable wheel robot with a passive leg," in *Intelligent Robots and Systems (IROS)*, 2015 IEEE/RSJ International Conference. IEEE, pp. 4165-4170.

[11] Lee, D. Jung, G. Sin, M. Ahn S. & Cho, K. (2013). "Deformable Wheel Robot Based on Origami Structure," in *IEEE International Conference on Robotics and Automation*, Karlsruhe, Germany.

[12] Sun, T. Xiang, X. Su, W. Wu, H. & Song, Y. (2017). "A transformable wheel-legged mobile robot," *Design, analysis and, Robotics and Autonomous Systems*, vol. 98, pp. 30-41.

[13] Chatzakis, J., Kalaitzakis, K., Voulgaris, N. C., & Manias, S. N. (2003). "Designing a new generalized battery management system," *IEEE transactions on Industrial Electronics*, 50(5), 990-999.

[14] Kim, Y. Jung, G. Kim, H. Cho, K. & Chu, C. (2013). "Wheel transformer: A miniaturized terrain adaptive robot with passively transformed wheels," in *Robotics and Automation (ICRA)*, IEEE International Conference on. IEEE, pp. 5625-5630.

[15] Raza, K. Masoom, K. Kamil, M. & Kumar, P. (2016). "Speed Control of DC Motor by using PWM," *International Journal of Advanced Research in Computer and Communication Engineering 5.4*.

[16] Petru, M. Livinti, S. & Mazen, G. (2015). "PWM control of a DC motor used to drive a conveyor belt," *Procedia Engineering 100*, pp299-304.

[17] Johnson, M. & Moradi, M. (2005). "PID control," London, UK: Springer-Verlag London Limited.

[18] Visioli, A. (2006). "Practical PID control," Springer Science and Business Media.

[19] Li, Y. Heong Ang, K. & Chong, G. (2006). "PID control system analysis and design," IEEE Control Systems Magazine 26.1: 32-41.

[20] Bhardwaj, J. Rashmi, K. & Datta, D. (2020). "Consensus algorithm," *Decentralised Internet of Things*. Springer, Cham, 91-107.

[21] Liu, K., Li, K., Peng, Q., & Zhang, C. (2019). "A brief review on key technologies in the battery management system of electric vehicles," *Frontiers of mechanical engineering*, 14, 47-64.

[22] Lelie, M., Braun, T., Knips, M., Nordmann, H., Ringbeck, F., Zappen, H., & Sauer, D. U. (2018). "Battery management system hardware concepts: An overview," *Applied Sciences*, 8(4), 534.